

Potential Barrier Classification by Short-Time Measurement

Er'el Granot*

*Department of Electrical and Electronics Engineering,
College of Judea and Samaria, Ariel, Israel*

Avi Marchewka†

*Kibbutzim College of Education
Ramat-Aviv, 104 Namir Road 69978 Tel-Aviv, Israel*

(Dated: November 15, 2018)

We investigate the short-time dynamics of a delta-function potential barrier on an initially confined wave-packet. There are mainly two conclusions: A) At short times the probability density of the first particles that passed through the barrier is unaffected by it. B) When the barrier is absorptive (i.e., its potential is imaginary) it affects the transmitted wave function at shorter times than a real potential barrier. Therefore, it is possible to distinguish between an imaginary and a real potential barrier by measuring its effect at short times only on the transmitting wavefunction.

PACS numbers: 03.65.-w, 03.65.Nk, 03.65.Xp.

I. INTRODUCTION

One of the methods in imaging a turbid or a diffusive medium with optical radiation is the time-gating technique [1, 2, 3, 4, 5]. In this technique a temporally narrow pulse is injected into the medium. Owing to the diffusivity of the medium, when the pulse exits the medium it becomes considerably wider. However, if the first arriving photons are separated from the rest of the pulse then it is possible to use these, so called, ballistic (or quasi ballistic) photons to reconstruct the ballistic image of the medium.

Therefore, by employing a short time-gating technique the multi-scattering effect can be eliminated. Indeed, such methods were employed in recognizing hidden objects and informative signals in diffusive media [6]. Naively, one might expect that this technique can be implemented for electron imaging to "see" absorptive objects inside scattering medium. That is, one can send a short pulse of electrons to one end of the medium, while at the other end only the first arriving electrons will be measured. By doing so all the noise caused by the multi-scattering should be eliminated. On the other hand, the presence of absorptive regions (like imaginary potentials [7]) will be felt in the amount of the early arriving electrons. However, electrons are governed by the Schrödinger equation, and unlike the Maxwell wave-equation, has a parabolic dispersion relation. As a consequence, any localized wave-packet suffers from strong dispersion, since each spectral component propagates at different velocity. The fastest particles are the most en-

ergetic ones, which pass through the medium unaffected, since the barrier's potential energy is negligible compared to their kinetic energy. In particular, when the medium is a certain barrier (or well), we conclude that when only the first-arriving particles are measured there should be no trace of the barrier's presence. It does not matter what shape or height the barrier has - the first particles that pass through the barrier should be indifferent to it. Thus, one may argue that the time-gating technique cannot be implemented to electrons imaging, at least not in its naive form. However, we show that the short-time measurement reveals information about the nature of the barrier - whether it is imaginary or real.

There is a peculiar distinction between an absorbing medium (e.g., an imaginary potential) and a non-absorbing one (e.g., a real potential). While they both have no effect on the wavepacket (both transmitted and reflected) at $t \rightarrow 0$, the imaginary barrier influences the wavepacket sooner. In other words, in the temporal Taylor expansion of the probability density the imaginary potential appears at smaller order than a real potential. It is then clear that we can classify the barrier as an absorptive one simply by measuring the wave-packet at short times. Note that in general it is required to measure both reflection and transmission coefficients to figure out if the barrier is absorptive or not.

Recently [8], it has been demonstrated even experimentally that it is feasible to investigate the 1D scattering of a Bose-Einstein condensate by a narrow defect. Therefore, it seems that there is a good chance of witnessing these effects in the laboratory in the near future.

In this paper we demonstrate this effect rigorously (both analytically and by a numerical simulation) for the delta function potential. That is, we show that it is possible to identify an absorptive potential by measuring the short time dynamics of only the transmitted wavefunc-

*Electronic address: erel@yosh.ac.il

†Electronic address: marchew@post.tau.ac.il

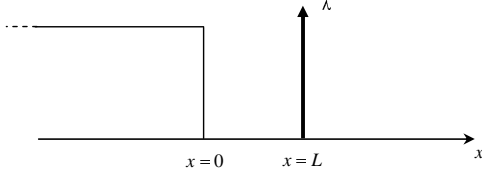


FIG. 1: *System schematic: a semi-infinite wavepacket hitting a delta function potential.*

tion.

The initial state we consider is a wave-packet, which is confined to one side of the barrier. It is then demonstrated that the wavefunction at the other side is independent of the barrier for short times, while the temporal dependence depends on the exact nature of the barrier (absorptive or not).

II. SYSTEM DESCRIPTION AND DYNAMICS

Evidently, in order to confine the initial wavepacket to one side of the barrier, there has to be a certain singularity in the wavepacket. In this paper we focus on a step function to simplify the problem; however, it has been demonstrated elsewhere that most of the conclusions are valid even in the continuous case provided the measurements are taken at specific ranges (see ref.[9]). Is is also

demonstrated at the end of the paper that the main conclusions are valid even when the initial wavepacket is a Gaussian. For simplicity we take a 1D delta function as the potential barrier.

The system illustration is depicted in fig.1. Initially, the wave packet has the form [7, 9, 10]

$$\psi(x, t = 0) = \theta(-x) \exp(ik_0 x) \quad (1)$$

and a distance L from its front we place a delta-function barrier $V(x) = \lambda \delta(x - L)$ (see fig.1). That is, the Schrödinger equation reads

$$-\frac{\partial^2}{\partial x^2} \psi + \lambda \delta(x - L) \psi = i \frac{\partial \psi}{\partial t} \quad (2)$$

therefore for $t > 0$

$$\psi(x, t) = \frac{1}{2\pi} \int dk \varphi(k) \chi(k, x) \exp(-ik^2 t) \quad (3)$$

where

$$\varphi(k) = \frac{i}{k - k_0 + i0} \quad (4)$$

is the Fourier transform of $\psi(x, t = 0)$ and

$$\chi(k, x) \equiv \exp(ikx) + \frac{i\lambda/2}{k - i\lambda/2} \exp(ik|x - L| + ikL) \quad (5)$$

The general solution is (for $x > 0$)

$$\psi(x, t) = \frac{e^{ix^2/4t}}{2} w \left[\sqrt{it} \left(\frac{x}{2t} - k_0 \right) \right] + \frac{e^{iy^2/4t}}{2} \frac{i\lambda/2}{k_0 - i\lambda/2} \left\{ w \left[\sqrt{it} \left(\frac{y}{2t} - k_0 \right) \right] - w \left[\sqrt{it} \left(\frac{y}{2t} - i\frac{\lambda}{2} \right) \right] \right\} \quad (6)$$

where $w(z) \equiv \exp(-z^2) \text{erfc}(-iz)$ [11] and $y \equiv L + |x - L|$. In short times one can expand this expression in powers of t . Up to $t^{5/2}$

$$\psi(x, t) \simeq \sqrt{\frac{it}{\pi}} \frac{e^{ix^2/4t}}{x} \left[1 + \frac{2(k_0 x - i)}{x^2} t + \frac{4(k^2 x^2 - 3ik_0 x - 3)}{x^4} t^2 \right] + \frac{(it)^{3/2}}{\sqrt{\pi}} \frac{e^{iy^2/4t}}{y^2} \lambda \left[1 + \frac{i(\lambda y - 6) + 2k_0 y}{y^2} t \right] \quad (7)$$

for $x > L$

$$\psi(x, t) \simeq \sqrt{\frac{it}{\pi}} \frac{e^{ix^2/4t}}{x} \left[1 + \frac{2(k_0 x - i)}{x^2} t + \frac{4(k^2 x^2 - 3ik_0 x - 3)}{x^4} t^2 + \frac{i\lambda}{x} t - \frac{\lambda(\lambda x - 6 - 2ik_0 x)}{x^3} t^2 \right]$$

and to the third order of t :

$$|\psi(x > L, t)|^2 \simeq \frac{t}{\pi x^2} \times \left\{ 1 + 4 \frac{k_0 t}{x} + 4 \frac{3(k_0 x)^2 - 5}{x^4} t^2 + \frac{\lambda}{x^2} t^2 \left(\frac{8}{x} - \lambda \right) \right\} \quad (8)$$

we can see that the barrier's presence is felt only at the third order of t .

Even when $k_0 \ll \lambda$ and $x \rightarrow \infty$ the barrier's presence has a significant influence when the measurement is taken in the range $4k_0 x / \lambda^2 \ll t \ll x / \lambda$.

On the other hand, for $0 < x < L$, owing to the

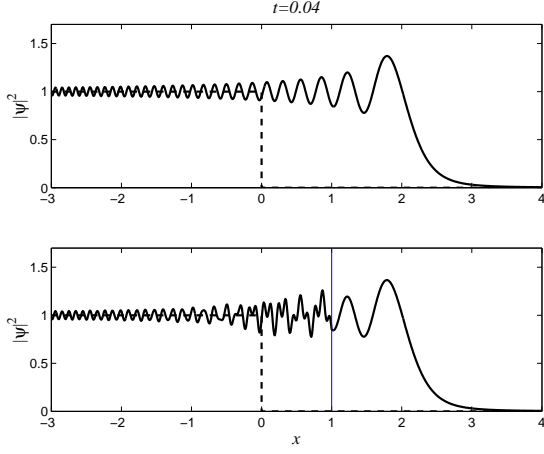


FIG. 2: A comparison between the solution with (lower panel) and without (upper panel) the barrier, which is represented by the horizontal line at $x = 1$. The initial state is represented by the dashed line. The parameters in this case are $L = 1$, $k_0 = 30$, $t = 0.04$ and $\lambda = 3$.

reflection from the barrier, the probability density's dependence on the barrier appears even in the $t^{3/2}$ order.

$$\psi(x, t) \simeq \sqrt{\frac{i}{\pi}} \frac{e^{ix^2/4t}}{x} \left[t^{1/2} + \frac{2t^{3/2}}{x} \left(k_0 + \frac{i}{x} \right) \right] + i\lambda \sqrt{\frac{i}{\pi}} \frac{e^{i(2L-x)^2/4t} t^{3/2}}{(2L-x)^2} \quad (9)$$

and

$$|\psi(x, t)|^2 \simeq \frac{t}{\pi} \times \left\{ \frac{1}{x^2} \left[1 + \frac{4tk_0}{x} \right] - \frac{2\lambda t}{x(2L-x)^2} \sin \left[\frac{L(L-x)}{t} \right] \right\} \quad (10)$$

That is, the dependence appears at the probability density at the coefficient of t^2 .

Obviously, this approximation applies only when the argument $L(L-x)/t$ is not too small.

In Fig.2 we plot a comparison between the propagation of the wavepacket in case the barrier is absent (upper panel) and when it is present (lower panel). In Fig.3 the difference between the two (with and without the barrier, i.e., $\Delta|\psi|^2 = |\psi|_{with}^2 - |\psi|_{without}^2$) is plotted. Despite the fact that the packet passes *through* the potential, its effect beyond the barrier $x > L$ is miniscule and for $|x|^2 \gg 1$ the two solutions are essentially identical.

Moreover, the difference between the $x > L$ and $x < L$ regimes is clear from the figure. In the latter regime the influence of the potential is felt for longer distances, but still when $\frac{|x|^2}{t} \rightarrow \infty$ its influence decays to zero.

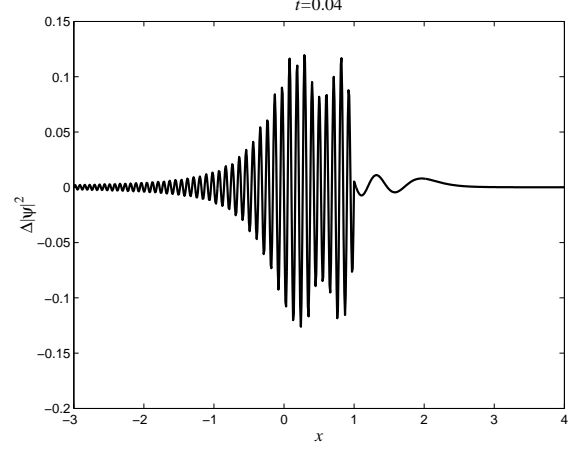


FIG. 3: : The difference between the solution when the barrier is present and when it is absent. Clearly, as $|x|^2/t \gg 1$ the two solutions are identical.

When the potential is absorptive the Schrödinger equation should be rewritten

$$-\frac{\partial^2}{\partial x^2} \psi + i\lambda \delta(x-L)\psi = i\frac{\partial \psi}{\partial t} \quad (11)$$

$$\psi(x, t) = \sqrt{\frac{it}{\pi}} \frac{e^{ix^2/4t}}{x} \left[1 + \frac{2(k_0 x - i) - \lambda x}{x^2} t + O(t^2) \right] \quad (12)$$

and the probability density satisfies

$$|\psi(x > L, t)|^2 = \frac{t}{\pi x^2} \left\{ 1 + 2 \frac{2k_0 - \lambda}{x} t + O(t^2) \right\}. \quad (13)$$

In this case the potential presence appears in the probability density at the second order of t (and not the third as in eq.8).

In the case where the wavefunction initially vanishes at $x = 0$ ([9, 10, 12]), e.g., when

$$\psi(x, t = 0) = \theta(-x) \sin(k_0 x) \quad (14)$$

The general solution is

$$\begin{aligned} \psi(x, t) = & \frac{e^{ix^2/4t}}{4i} w \left[\sqrt{it} \left(\frac{x}{2t} - k_0 \right) \right] + \frac{e^{iy^2/4t}}{4} \frac{\lambda/2}{k_0 - i\lambda/2} \left\{ w \left[\sqrt{it} \left(\frac{y}{2t} - k_0 \right) \right] - w \left[\sqrt{it} \left(\frac{y}{2t} - i\frac{\lambda}{2} \right) \right] \right\} \\ & - \left\{ \frac{e^{ix^2/4t}}{4i} w \left[\sqrt{it} \left(\frac{x}{2t} + k_0 \right) \right] - \frac{e^{iy^2/4t}}{4} \frac{\lambda/2}{k_0 + i\lambda/2} \left\{ w \left[\sqrt{it} \left(\frac{y}{2t} + k_0 \right) \right] - w \left[\sqrt{it} \left(\frac{y}{2t} - i\frac{\lambda}{2} \right) \right] \right\} \right\} \end{aligned} \quad (15)$$

In short times one can expand this expressions in powers of t .
Up to $t^{5/2}$

$$\begin{aligned} \psi(x, t) \simeq & -\sqrt{\frac{i}{\pi}} \frac{2k_0 t^{3/2} e^{ix^2/4t}}{x^2} \left[i + \frac{6}{x^2} t \right] \\ & + \sqrt{\frac{i}{\pi}} \frac{2k_0 t^{5/2} e^{iy^2/4t}}{y^3} \lambda \end{aligned} \quad (16)$$

for $x > L$

$$\psi(x, t) \simeq \frac{t^{3/2}}{\sqrt{i\pi}} \frac{e^{ix^2/4t}}{x^2} 2k_0 \left[1 + \frac{it}{x} \left(\lambda - \frac{6}{x} \right) \right] \quad (17)$$

and

$$|\psi|^2 \simeq \frac{4k_0^2 t^3}{\pi x^4} + O(t^4) \quad (18)$$

we can see that the barrier is not felt even at the third order of t .

Although the phase of ψ , "feels" the barrier even in the first order of t , the leading term is proportional to t^{-1}

$$\angle \psi \simeq -\frac{\pi}{4} + \frac{x^2}{4t} + (x\lambda - 6) \frac{t}{x^2}. \quad (19)$$

III. THE CONTINUOUS CASE: GAUSSIAN DYNAMICS

The fact that we used singular initial wavefunction may raise skepticism about the physical validity of

the conclusions. However, the main conclusions of the semi-infinite plane wave can be deduced even when the initial wavepacket is a continuous wavefunction, such as a Gaussian. However, owing to the finite spectral width of the Gaussian, high energy particles are very rare in the packet, and therefore the reasoning that was used in the semi-infinite plane wave can be used only in the intermediate temporal region and fails at $t \rightarrow 0$. Therefore, we should expect to find the same conclusions in a certain intermediate period (as in ref. [9]).

If the initial wavepacket is a Gaussian:

$$\psi(x, t=0) = \sqrt{\frac{2}{\pi}} \frac{1}{\sigma} \exp \left\{ -\left(\frac{x}{\sigma} \right)^2 + ik_0 x \right\} \quad (20)$$

then

$$\begin{aligned} \psi(x > L, t \geq 0) = & \\ \frac{1}{\sqrt{2\pi}} \int dk & \frac{\exp \left\{ -(k - k_0)^2 \sigma^2/4 + ikx - ik^2 t \right\}}{1 - i\lambda/2k} \end{aligned} \quad (21)$$

the general solution is

$$\psi(x > L, t \geq 0) = \left\{ \frac{1}{\sqrt{2\pi}s} - \frac{\lambda}{\sqrt{8}} w \left[i \frac{\lambda s}{2} - \frac{[\sigma^2 k_0/2 + ix]}{2s} \right] \right\} \exp \left\{ \frac{1}{4} \frac{[\sigma^2 k_0/2 + ix]^2}{s^2} - \frac{\sigma^2 k_0^2}{4} \right\} \quad (22)$$

where $s \equiv \sqrt{\sigma^2/4 + it}$. For short times

$$\psi(x > L, t \geq 0) \simeq \frac{1}{\sqrt{2\pi}s} \frac{1}{1 - i \frac{\lambda s^2}{\sigma^2 k_0/2 + ix}} \exp \left\{ \frac{1}{4} \frac{[\sigma^2 k_0/2 + ix]^2}{s^2} - \frac{\sigma^2 k_0^2}{4} \right\} \quad (23)$$

where for large distances $x + L \gg \sigma^2 k_0$ can be approxi-

mated in the two extreme cases: $t \ll \sigma^2/4$ and $t \gg \sigma^2/4$.

In the former case

$$\psi(x > L, t \geq 0) = \frac{\sqrt{2}}{\sqrt{\pi}\sigma} \frac{1}{1 - \frac{\lambda\sigma^2}{4x}} \exp\left\{-\frac{x^2}{\sigma^2}\right\} \quad (24)$$

the barrier influence is independent of time, and in fact, very far from the barrier $x \gg \lambda\sigma^2$ the barrier's influence is negligible. However, we see here that in the limit $t \rightarrow 0$, due to the finite spectral width $\sim \sigma$, the presence of the barrier is always felt. (Note that the singular case $4x = \lambda\sigma^2$ is not consistent with the above approximation). This is to be expected, since in a Gaussian distribution the number of particles with extremely large energies is exponentially small.

When $t \gg \sigma^2/4$

$$\psi(x > L, t \geq 0) = \frac{1}{\sqrt{2\pi it}} \frac{1}{1 - i\frac{\lambda t}{x}} \exp\left\{\frac{i}{4} \frac{x^2}{t} - \frac{\sigma^2 k_0^2}{4}\right\}$$

we recognize a penetration velocity. When $x/t \ll \lambda$ the barrier has a large impact, however, if the particles' velocity is very large $x/t \gg \lambda$ the barrier's influence is negligible.

And similarly, in the temporal period $\sigma^2/4 \ll t \ll x/\lambda$ the difference between real and imaginary barrier is apparent. For a real barrier

$$|\psi(x > L, t > 0)|^2 \cong \frac{1 - (\lambda t/x)^2}{2\pi t} \exp\left\{-\frac{\sigma^2 k_0^2}{4}\right\} \quad (25)$$

while for an imaginary one

$$|\psi(x > L, t > 0)|^2 \cong \frac{1 - 2\lambda t/x}{2\pi t} \exp\left\{-\frac{\sigma^2 k_0^2}{4}\right\} \quad (26)$$

Again, the the influence of the absorptive potential appears in a lower order term.

IV. SCHEMATIC EXPERIMENTAL REALIZATION

One of the methods of emphasizing the impact of the potential is by placing the potential barrier (delta function in our case) in one arm of a Mach-Zehnder interferometer (see fig.4).

Let us denote by c_1 and ic_2 the transmission and reflection coefficients of each of the two interferometers' beam splitters (BS1 and BS2 in figure.4). With this notation we assume (without loss of generality) that both c_1 and c_2 are real and conservation of energy implies $c_1^2 + c_2^2 = 1$.

$$\psi(x, t) = \sqrt{\frac{it}{\pi}} \frac{e^{ix^2/4t}}{x} \left\{ \left[1 + \frac{2(k_0 x - i)}{x^2} t + \frac{4(k_0^2 x^2 - 3ik_0 x - 3)}{x^4} t^2 \right] (c_1^2 - c_2^2) + \left[\frac{i\lambda}{x} t - \frac{\lambda(\lambda x - 6 - 2ik_0 x)}{x^3} t^2 \right] c_1^2 \right\}$$

Let us further assume that both BS's are almost 50:50, i.e., $c_1^2 = 0.5(1 - \varepsilon)$, $c_2^2 = 0.5(1 + \varepsilon)$ and $\varepsilon \ll 1$. In this case, for short time

$$\psi(x, t) \simeq \sqrt{\frac{it}{\pi}} \frac{e^{ix^2/4t}}{x} \left(\varepsilon + \frac{i\lambda}{2x} t \right) \quad (27)$$

and the probability density can be approximated

$$|\psi(x, t)|^2 \simeq \frac{t}{\pi x^2} \left[\left(\varepsilon - \frac{\Im \lambda}{2x} t \right)^2 + \left(\frac{\Re \lambda}{2x} t \right)^2 \right] \quad (28)$$

Thus, when the potential is real the potential-dependent term has a cubic dependence on time

$$|\psi(x, t)|^2 \simeq \frac{t}{\pi x^2} \left[\varepsilon^2 + \left(\frac{\lambda}{2x} t \right)^2 \right] \quad (29)$$

while if the potential is imaginary the temporal dependence of the potential-dependent term is parabolic

$$|\psi(x, t)|^2 \simeq \frac{t\varepsilon}{\pi x^2} \left[\varepsilon - \frac{\Im \lambda}{x} t \right] \quad (30)$$

To emphasize the difference we define $\Delta|\psi|^2 \equiv |\psi|^2 - |\psi|_{free}^2$ as the difference between the probability density at the interferometer exit when the barrier is present ($|\psi|^2$) and when it is absent ($|\psi|_{free}^2$).

In fig.5 we plot the temporal evolution of $\Delta|\psi|^2$, which is measured at the exit of the interferometer (at $x = 10$ from the barrier) for the two cases (real and imaginary potentials). The only difference between the two plots is the potential ($i\lambda$ instead of λ). While the two plots are similar after long times, their temporal differences are considerably different for short times as eqs. 29 and 30 imply (like t^3 and t^2 respectively).

V. SUMMARY

The short-time influence of a delta-function potential barrier on an initially confined wave-packet was investigated. It was shown that at short times the barrier presence has a negligible influence, if any, on the wavepacket

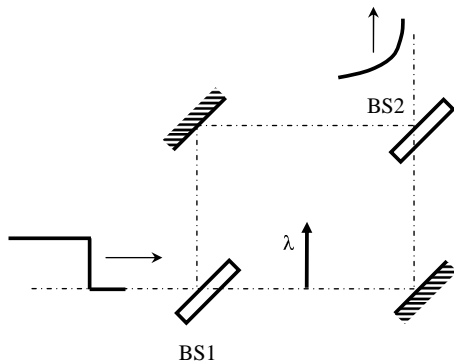


FIG. 4: schematic illustration of a Mach-Zehnder interferometer for barrier classification.

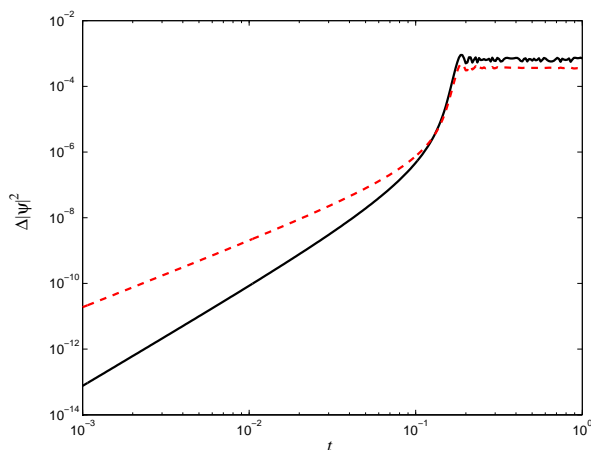


FIG. 5: The temporal evolution of $\Delta|\psi|^2$ outside the interferometer (a distance $x = 10$ from the barrier) for a real potential (solid line) and an imaginary one (dashed line). $c1 = \sqrt{0.49}$ and the other system's parameters are the same as in fig.2

dynamics. This result applies also for the probability density of the particles that passed through the barrier. It was also demonstrated that at short times an absorptive barrier (i.e. imaginary) has a different impact on the dynamics than a non-absorptive (i.e., real) one. Namely, at short times an absorptive barrier appears at the coefficient of the t^2 term, while a non absorptive barrier appears only at the coefficient of the t^3 term. Therefore, it is possible to distinguish between an imaginary and a real potential barrier by measuring its effect at short times only on the transmitting wavefunction. There is no need to measure the transmission and reflection coefficient simultaneously.

-
- [1] P.Naulleau, E. Leith, H. Chen, B. Hoover, and J. Lopez, *Appl. Opt.* **36** 3889 (1997).
 - [2] J. C. Hebden and D.T. Delpy, *Opt. Lett.* **19** 311 (1994).
 - [3] G. M. Turner, G. Zacharakis, A. Soubret, J. Ripoll, V. Ntziachristos, *Opt. Lett.* **30** 409 (2005).
 - [4] A. Ya. Polishchuk, J. Dolne, F. Liu, and R. R. Alfano, *Opt. Lett.* **22** 430 (1997).
 - [5] L. Wang, X. Liang, P. Galland, P. P. Ho, and R. R. Alfano, *Opt. Lett.* **20** 913 (1995).
 - [6] M. Paciaroni and M. Linne, *Appl. Opt.* **43** 5100 (2004).
 - [7] J.G. Muga, J.P. Palao, B. Navarro, I.L. Egusquiza. *Phys. Reports* **395**(2004).
 - [8] C. Fort, L. Fallani, V. Guarrera, J. E. Lye, M. Modugno, D.S. Wiersma, and M. Inguscio, *Phys. Rev. Lett.* **95** 170410 (2005).
 - [9] E. Granot, A. Marchewka, *Europhys. Lett.*, **72** (3), p.1 (2005).
 - [10] M. Moshinsky, *Phys. Rev.* **88**, p.625 (1952); M. Kleber, *Phy. Rep.*, pp.236-331 (1994); G. Garcia-Calderon, J. Villavicencio and N. Yamada, *Phys. Rev. A* **67**, 042111 (2003); M. Moshinsky, *Am. J. Phys.* **44**, p.1037 (1976);
 - [11] M. Abramowitz and I.A. Stegun, *Handbook of Mathematical Functions* (Dover, New York) 1972.
 - [12] S. Godoy, *Phys. Rev. A* **65**, 042111 (2002)